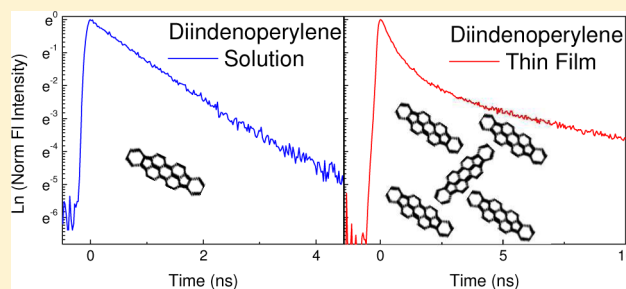


Excited-State Dynamics of Diindenoperylene in Liquid Solution and in Solid Films

Valerie M. Nichols,[†] Katharina Broch,^{‡,§} Frank Schreiber,[‡] and Christopher J. Bardeen^{*,†}[†]Department of Chemistry, University of California, Riverside, Riverside, California 92521, United States[‡]Institute for Applied Physics, Eberhard-Karls Universität Tübingen, 72076 Tübingen, Germany

ABSTRACT: The excited-state dynamics of diindenoperylene (DIP) are investigated in dilute solution and in a solid film at room temperature using picosecond photoluminescence and femtosecond transient absorption measurements. In solution, DIP undergoes a rapid (0.89 ns) internal conversion back to its ground state, with no detectable formation of triplet or other long-lived states. In the solid state, multiple emissive species are formed. The time-resolved photoluminescence signal is dominated by an intrinsic exciton that decays on a time scale of 166 ps. Emission from lower energy excimer-like species then persists for >10 ns. Transient absorption experiments indicate that the majority of the excited-state population relaxes to the ground state on the 166 ps time scale, but a smaller fraction (<10%) survives in longer-lived trap or defect states. The rapid internal conversion leads to transient heating that results in a derivative line shape in the transient absorption signal at longer delays. DIP does not appear to support long-lived singlet exciton states or singlet fission. The implications of these results for the function of DIP in organic solar cells are discussed.



INTRODUCTION

Organic molecular semiconductors are used in electronic devices ranging from transistors to solar cells. One advantage of organic semiconductors is the variety of molecular structures and interfaces that can give rise to different material properties.¹ The rylene family comprises a class of molecules that crystallize easily, have high stability, and support long exciton and charge carrier diffusion lengths. Diindenoperylene (DIP), whose structure is shown in Figure 1, is an extended rylene whose solid-state thin films have been extensively studied.^{2–12} Its high degree of order, coupled with its excellent charge transport properties, have made it an increasingly popular choice as a component of organic photovoltaic (OPV) devices.^{13–16}

Furthermore, DIP has the ability to form crystalline mixtures with other conjugated molecules like perfluoropentacene or pentacene, opening up the possibility of making well-defined composite materials.^{17–21} Despite its use in OPVs, much remains unclear in terms of DIP's basic photophysics. Since DIP's contribution to the photocurrent in an OPV should be determined at least in part by its exciton diffusion length, which in turn is determined by its excited-state lifetime, an improved understanding of its molecular photophysics is important for understanding how this material functions in an OPV.

In this paper, we investigate the excited-state dynamics of DIP in both dilute solution and in a polycrystalline solid film at room temperature. In solution, DIP undergoes internal conversion back to the ground state on a subnanosecond time scale. This rapid internal conversion, seen in other acene molecules that incorporate a five-membered ring, has been attributed to a lack of resonance stabilization.^{22,23} In solid form, DIP exhibits a complex decay that involves multiple emitting species. The time-resolved photoluminescence (PL) signal is dominated by the intrinsic exciton decay on a time scale of 170 ps. Emission from lower energy excimer-like species then persists for >10 ns. Our results suggest that despite its herringbone crystal motif, DIP does not support phenomena like long-lived singlet exciton states (as in crystalline anthracene^{24,25}) or singlet fission (as in crystalline perylenes,^{26,27} tetracene,^{28,29} and pentacene^{30–32}) seen in crystals

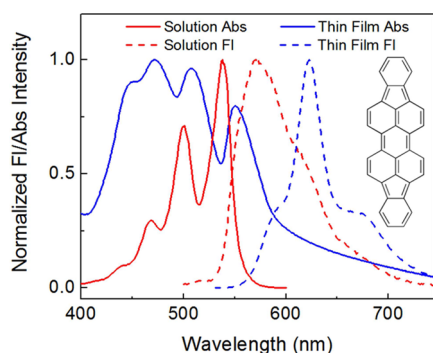


Figure 1. Absorption (solid) and fluorescence (dotted) spectra of DIP monomer in benzene (red) and 100 nm thick thin films (blue). The molecular structure of DIP is also shown.

Received: April 7, 2015
Revised: May 20, 2015
Published: May 20, 2015

with similar packing motifs. Instead, rapid internal conversion leads to transient heating, with a small fraction (<10%) of the excitons surviving in longer-lived trap or defect states. We hypothesize that DIP's success in OPV applications stems largely from its ordered packing in thin films and high charge carrier mobilities, as opposed to its excitonic contributions.

EXPERIMENTAL SECTION

Diindenoperylene was purchased from PAH Greifenwald and purified using gradient sublimation. Liquid solution samples of DIP were made by dissolving the solids in acetonitrile, toluene, chlorobenzene, and benzene at 10^{-5} – 10^{-6} M concentrations. All solvents were purchased from Sigma-Aldrich (HPLC grade, >99.9%) and were used as received.

Solid-state films of DIP with thicknesses of 100 nm were prepared using organic molecular beam deposition. The SiO₂ and glass substrates were ultrasonically cleaned with acetone, isopropyl alcohol, and deionized water for 5 min each and dried on a heater to remove water. The substrates were glued on a sample holder using silver paste, which was dried again on a heater. Afterward, the substrates were loaded into a vacuum chamber and kept for 8 h at a pressure of 10^{-6} mbar and a temperature of 120 °C to remove residual water and solvents. After transfer in the UHV-growth chamber (base pressure of 2×10^{-10} mbar) without breaking the vacuum, the samples were kept at 300 °C for 10 min as a last cleaning step. Finally, the samples were cooled down to 25 °C, and the film growth was started after the substrate temperature was stable. The films were deposited at a rate of 2 Å/min simultaneously on two quartz glass substrates and a Si(100) substrate with a native oxide layer of 2 nm thickness. The thickness of the samples was determined using a quartz crystal microbalance calibrated using X-ray reflectivity and confirmed by ellipsometry based on the previously determined optical constants of DIP.³³

Absorption spectra of liquid samples were taken in a 1 cm quartz cuvette in a Cary 50 spectrometer. To avoid quenching by O₂, samples were sealed in a 1 cm quartz cuvette with an overpressure of argon after being bubbled under argon for 15 min. Steady-state fluorescence spectra were measured under vacuum in a Janis ST100 cryostat with a Fluorolog 3 spectrofluorimeter with 400 nm excitation and front face detection. Absorption of thin film samples were also measured for the samples in the cryostat, using a Cary 500 spectrometer.

Fluorescence lifetime data were taken using front face detection with a Hamamatsu C4334 StreakScope picosecond streak camera with a time resolution of 15 ps. The 400 nm excitation pulse was generated by frequency doubling the 800 nm pulse from a 1 kHz Coherent Libra Ti:sapphire regenerative amplifier. Scattered pump light was removed by placing a 450 nm long wave pass filter and 420 nm color filter on the input lens before the streak camera. The fluorescence was detected at 54.7° relative to the pump to eliminate rotational diffusion effects. The pulse fluences were kept below 1.9 μJ/cm², and measurements of the fluorescence decay at different laser intensities yielded similar decays, indicating that exciton–exciton annihilation did not influence the results.

Transient absorption (TA) experiments were performed using a 1 kHz Coherent Libra Ti:sapphire regenerative amplifier with an Ultrafast Systems Helios transient absorption spectrometer. The 400 nm pump pulse was generated by frequency doubling the 800 nm Libra output, and the white light continuum probe was generated by focusing a small portion of the 800 nm fundamental into a sapphire plate. The

pump and probe were focused onto the same spot of the sample, and the transmitted probe beam was focused into an optical fiber coupled to an Ocean Optics S2000 spectrometer. The spectrometer and motorized delay stage were controlled with the Helios software. The motorized stage allows for a delay of up to 1.6 ns. In order to look at longer time dynamics, additional time delays up to 7 ns could be generated by manually translating a separate set of mirrors on the laser table. Pump fluences ranged from 0.80 to 8.3 mJ/cm². Excitation densities ranged from 7.8×10^{18} to 7.9×10^{19} cm⁻³. The sample showed no sign of damage at these laser fluences.

RESULTS AND DISCUSSION

The absorption line shape of DIP in solution (Figure 1) has a vibronic progression that resembles those of smaller members of the rylene family, like perylene and peropyrene.³⁴ The increased conjugation leads to a red shift of about 100 nm relative to those molecules, with the lowest energy peak located at 540 nm. A more profound difference is that DIP's fluorescence spectrum does not mirror its absorption but is broadened with a different vibronic intensity pattern. Schael and Lohmansroben deduced that the emission originated from an electronic state that was different from the absorbing state, with a lower oscillator strength that leads to a radiative lifetime of 58 ns.³⁵ This state also has a low fluorescence quantum yield, on the order of 1–2%. The low yield results from a rapid fluorescence decay. Figure 2 shows the fluorescence decay in

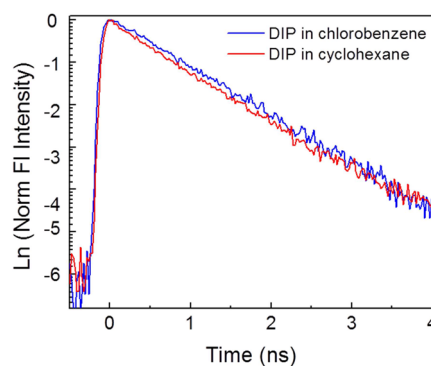


Figure 2. Normalized fluorescence decays of DIP in chlorobenzene (blue) and cyclohexane (red). The decays are single exponential with a lifetime of 890 ps in both solvents.

two solvents with different polarities: cyclohexane and chlorobenzene. The fluorescence decay was single exponential on all time scales with a lifetime of 0.89 ± 0.02 ns in all solvents tested, in good agreement with the value measured by Schael and Lohmansroben.³⁵

To confirm that the short fluorescence lifetime was due to rapid internal conversion, we used femtosecond transient absorption spectroscopy to look for evidence of the formation of other species (triplet, charge-transfer state) after the decay of the singlet state. These experiments were challenging due to the low solubility of DIP in common solvents, and benzene was eventually chosen to provide the highest concentration of 10^{-5} M. In Figure 3, we show the transient spectra at delays of 1 ps, 500 ps, 1 ns, and 7 ns. At 1 ps, the negative bleach signal at 540 nm overlaps a large induced absorption stretching from 600 nm well into the near-infrared. The time resolution of these experiments was limited to ~500 fs, and there is no further evolution of the TA spectrum after the pump pulse has finished

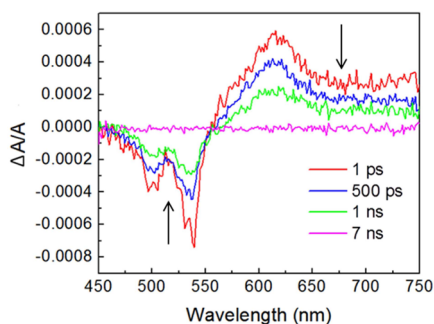


Figure 3. Transient absorption spectra $\Delta A/A$ for a 100 nm thick DIP crystalline thin film for probe pulse delays of 1 ps (red), 500 ps (blue), 1 ns (green), and 7 ns (pink). Black arrows indicate direction of spectral evolution with increasing time.

interacting with the sample. Thus, the relaxation from the initially excited bright state into the less emissive state that dominates the PL behavior must be complete within 1 ps. Note that this relaxation could not be resolved in our PL measurements due to the 15 ps time resolution of the streak camera system. After 1 ps, both the negative and positive TA signals decay with the same rate, and there is no sign of any new spectral features growing in. By 7 ns, there is no detectable TA signal, indicating that all the DIP molecules return to their ground state without forming long-lived intermediates. Given the triplet absorption coefficient is on the order of $40\,000\text{ M}^{-1}\text{ cm}^{-1}$, we should be able to detect even a few percent of this species if it were formed.³⁵ The TA delay line limited the time range over which the TA decays could be continuously measured, but over this limited time range, at all probe wavelengths, we found that the TA signals could be fit using a single exponential with a time constant fixed to 890 ps, the value extracted from the PL decays. In Figure 4 we show that both the bleach signal at 540 nm and the $S_1 \rightarrow S_n$ absorption at 720 nm decay with the same time kinetics.

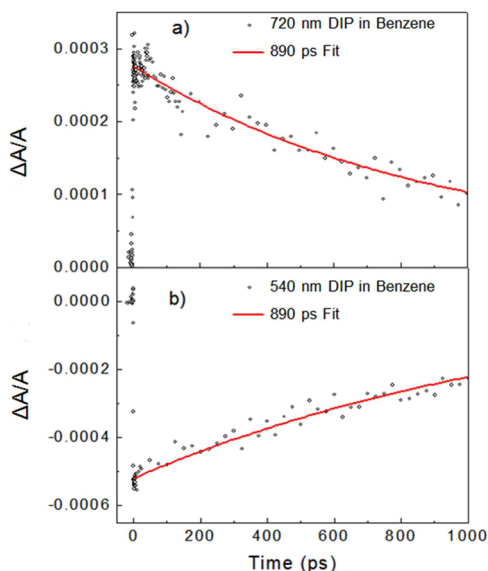


Figure 4. Experimental transient absorption signals (open circles) at (a) 720 nm and (b) 540 nm for DIP in benzene. Both traces can be fit to a single-exponential decay (red lines) of with a time constant of 0.89 ns, which agrees well with the fluorescence lifetime data.

In solution, DIP's photophysical behavior is determined by two sequential internal conversion processes. First, the initially excited singlet state quickly (<1 ps) relaxes to the lower lying singlet state. Some hint of a rapid, pulse-width-limited decay can be seen in the TA trace in Figure 4b, which probably reflects the subpicosecond relaxation to the lower singlet state. This state then relaxes back to the ground state via a second internal conversion process with the characteristic 890 ps decay time as determined by fitting the data in Figure 4. The behavior is similar to that of well-studied polyene systems in which the emission also takes place from a low-lying state, close in energy to the strongly allowed 1B_u state but possessing a much smaller transition dipole moment.^{36,37}

When DIP is deposited as a solid film on glass, its spectroscopic behavior changes significantly. On strongly interacting substrates like metal surfaces, DIP molecules tend to adopt a "lying down" configuration.^{12,38,39} On weakly interacting substrates like SiO_2 , the molecules tend to adopt a "standing up" configuration in the bulk,⁴⁰ although there is also evidence for some amount of "lying down" orientation, especially during the growth process at lower temperatures.^{9,41} The films in this study were deposited on glass substrates at room temperature, and it has been shown that such films have properties similar to those deposited on pristine SiO_2 .⁴² The absorption and fluorescence spectra of these DIP films are clearly different from those of DIP in dilute solution, as can be seen from Figure 1. The absorption and PL spectra of DIP are both red-shifted from those in solution. The absorption retains three distinct vibronic peaks, located at 560, 520, and 480 nm, but they are broadened by at least a factor of 2. The relative intensities of these peaks are similar, in contrast to the well-defined Franck–Condon progression seen in the monomer. The PL spectrum retains features that can be associated with vibronic structure, but whose relative intensities are completely different from those of the monomer.⁴³ The change in vibronic line shape can be taken as evidence for the formation of intermolecular exciton states.³³ The side-by-side herringbone packing motif, coupled with orientation of the transition dipole along the long axis of the molecule, would be expected to result in H-type aggregate states similar to what is observed in the oligothiophenes.^{44,45} In H-type aggregates, we expect to see a 0–0 peak that is reduced in intensity from the monomer, as observed experimentally.⁴⁶ However, as shown below, the steady-state PL actually consists of contributions from multiple emitting states. Because of these varied contributions, we did not attempt a detailed analysis of the PL line shape to determine the exact nature of the exciton state.

Heilig et al. studied the PL behavior of DIP thin films and deduced the presence of multiple emitting species that exhibited a complex temperature dependence.⁴⁷ They found that the PL decay at 300 K consisted of two components: an excitonic state with a lifetime of ~ 100 ps and a red-shifted, unstructured emission with an undetermined lifetime. In this paper, we concentrate on the room-temperature behavior, using a streak camera with 15 ps time resolution and 2 nm spectral resolution to measure the PL dynamics. As shown in Figure 5, the picosecond time-resolved PL experiments gave rise to multiexponential decays at all wavelengths, indicating the presence of several different emitting populations. In the 1 ns window, we found that $\sim 70\%$ of the singlet decayed with a 166 ps time constant, with an additional $\sim 30\%$ component with a time constant of 1.1 ns. Using a longer 20 ns time window (inset to Figure 5), we also identified a 6.4 ns decay component

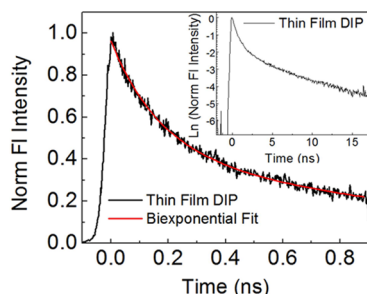


Figure 5. Normalized fluorescence decay of 100 nm thick DIP thin film in a 1 ns window on a linear scale. Overlaid in red is a biexponential decay fit with time constants of 166 ps and 1.1 ns. The inset shows the fluorescence decay from a 20 ns window on a log scale to show additional long-lived decay.

that has an amplitude of a few percent of the total. The bulk of the PL signal ($\sim 80\%$) decays within 1 ns (Figure 5). We do not see any rise in the PL signal at longer wavelengths that would indicate that the initial excited-state population is relaxing to lower energy emissive states. Instead, the different emitting states appear to decay independently.

The bright initial exciton state must relax either back to the ground state or to a dark excited state. One candidate for such a dark state is the triplet exciton, which could be formed by either rapid intersystem crossing or by singlet fission (SF). Since 166 ps is very rapid for intersystem crossing in the absence of heavy atoms, SF would be the most likely mechanism for rapid triplet formation.^{48,49} The overall profile of the decay curve in Figure 4 is reminiscent of the behavior of solid tetracene, where SF leads to a prompt fluorescence decay followed by a much longer-lived delayed fluorescence.²⁹ Given their similar their crystal packing, we suspected that SF might play some role in the singlet relaxation in DIP. But when the PL decay of DIP was analyzed in detail, clear differences emerged between the behavior of the two crystals. First, the slow component in tetracene is true delayed fluorescence, where the later time spectrum is identical to that of the prompt fluorescence. This is not the case for DIP, where the PL line shape evolves to be dominated by a low-energy peak, as shown in Figure 6. In tetracene, the delayed fluorescence arises from a dark triplet population that is interconverting with the bright singlets. The role of the triplet makes the fluorescence decay susceptible to the influence of a magnetic field.^{50,51} We found that application

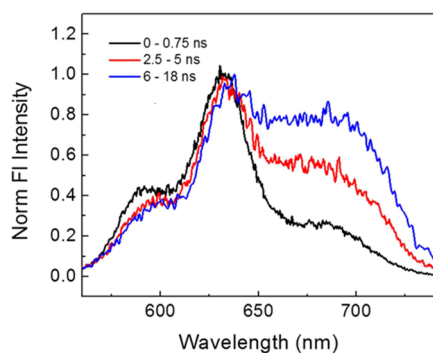


Figure 6. Normalized fluorescence spectra of DIP thin film integrated from 0 to 0.75 ns (black line), 2.5 to 5 ns (red line), and 6 to 18 ns (blue line). The intrinsic exciton peaks at 600 and 635 nm decay rapidly, leaving a red-shifted peak at around 690 nm dominant at later times.

of magnetic fields up to 7000 G had no observable effect on the DIP fluorescence decay. Finally, we did not observe a strong intensity dependence of the long-lived component of the decay, which would have been expected if it really results from a bimolecular recombination of triplet excitons. The decay of the delayed fluorescence in tetracene, on the other hand, does show a pronounced intensity dependence.^{52,53} SF in DIP would be significantly more uphill energetically than that in tetracene, since $2E(T_1) - E(S_1) = 2050 \text{ cm}^{-1}$ for the molecule in solution.³⁵ It may be that the energy barrier is sufficient to prevent SF in DIP, although the spectral line shapes (and thus the electronic structure of the singlet excitons) are also quite different from those observed in crystalline tetracene.

Since triplet formation and delayed fluorescence can be ruled out, the long-lived PL must originate from other singlet species. The broad peak at 690 nm that is prominent at later times in Figure 6 strongly suggests that the bulk of the long-lived states are excimers. The herringbone packing in a pristine DIP crystal would seem to preclude excimer formation, but structural defects can give rise to cofacial molecular arrangements that enable excimer formation, as observed in other herringbone crystals like anthracene.^{24,54,55} The lack of a pronounced rise time for the 690 nm feature suggests that the excimer emission arises from defect sites within the films that are directly excited by the laser.

In order to probe the ultimate fate of the DIP excited-state population, we turned to femtosecond TA experiments. These experiments again suffered from low signal levels. DIP tends to crystallize with its long axis close to perpendicular to the growth substrate.⁴⁰ Since its transition dipole moment is parallel to its long molecular axis, it cannot couple well to the incoming light field whose polarization is perpendicular to the surface normal. Nevertheless, we did obtain TA signals at relatively high pump pulse fluences. At these fluences, we saw clear evidence for exciton–exciton annihilation on the picosecond time scale. In Figure 7 we show the normalized decays of the DIP TA induced absorption signal, integrated over the range of 650–750 nm. The initial decay becomes much more rapid as the excitation density is increased from 10^{18} to 10^{19} cm^{-3} . By using a simple model for the exciton–exciton annihilation,^{53,56} we can derive an expression for the decay of the singlet population, $n_S(t)$:

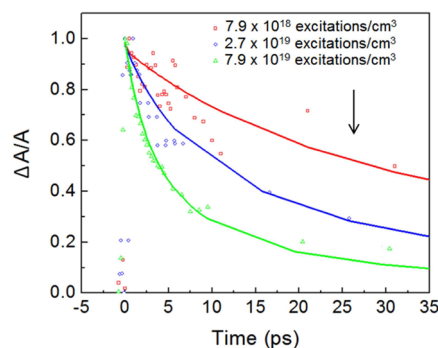


Figure 7. Early time transient absorption signal decays of a DIP thin film, integrated from 650 to 750 nm. The decays are measured at three different excitation densities: 7.9×10^{18} (red open squares), 2.7×10^{19} (blue open circles), and 7.9×10^{19} (green open triangles). The arrow indicates increasing excitation density. Overlaid in corresponding colors are exciton–exciton annihilation fits with $k_{ee} = 2 \times 10^{-9} \text{ cm}^3/\text{s}$ and $k_S = 6 \text{ ns}^{-1}$ (see eq 2).

$$\frac{\partial n_S}{\partial t} = -k_S n_S - k_{ee} n_S^2 \quad (1)$$

$$n_S(t) = \left[-\frac{k_{ee}}{k_S} + \left(\frac{1}{n_S(0)} + \frac{k_{ee}}{k_S} \right) e^{k_S t} \right]^{-1} \quad (2)$$

where k_S is the intrinsic singlet decay rate and k_{ee} is the exciton–exciton annihilation rate. If we fix $\tau_S = 1/k_S$ to be 170 ps, the value obtained from our early time PL decay, we can fit the curves in Figure 7 with $k_{ee} = 2 \times 10^{-9} \text{ cm}^3/\text{s}$. This value of k_{ee} is a factor of 5 smaller than those deduced for crystalline tetracene and β -perylene using a similar analysis.^{53,57} The small value of k_{ee} is surprising in light of the large exciton diffusion lengths reported for DIP, since k_{ee} should be directly proportional to the exciton diffusion constant.⁵⁸ However, in tetracene the singlet exciton is J-type,^{59–61} while in DIP it appears to be H-type. It is possible that the reduced oscillator strength of the H-type exciton either reduces its energy transfer rate or its radius of interaction. If this is the case, DIP would provide a good example of how exciton–exciton annihilation can be affected by the exciton’s electronic structure.

Once singlet exciton–exciton annihilation is taken into account, the subsequent evolution of the TA data is straightforward to analyze. The data at all wavelengths can be fit using a single-exponential decay with a time constant $\tau_S = 170$ ps and a constant offset. The necessity of the offset can be seen from the spectral data shown in Figure 8. At a delay of 1

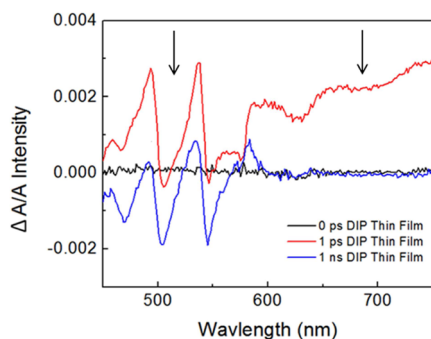


Figure 8. Transient absorption spectra of DIP thin film at probe pulse delays of 0 ps (before pump pulse, black), 1 ps (red), and 1 ns (blue). Black arrows indicate direction of spectral evolution with increasing probe delay.

ps, the signal is dominated by a broad induced absorption on which are superimposed sharp features located at 550, 520, and 480 nm, which we assign to the S_0 – S_1 bleach. The absorption decays with a time constant of $\tau_S = 170$ ps, but at a delay of 1 ns, the remaining signal has both positive and negative features that remain constant. The negative peaks at 550, 510, and 480 nm are close to the peaks in the steady-state absorption spectrum in Figure 1, but slightly blue-shifted. Furthermore, there are positive peaks between the negative peaks, and the signal overall has a derivative appearance rather than the appearance of a distinct excited-state absorption feature.

We consider two possible explanations for the behavior of the TA spectrum at long delays. The first possibility is that we are seeing the overlap of the bleach and the TA spectrum of a long-lived excited state produced by relaxation of the singlet. In this case, the S_0 – S_1 and the long-lived state absorption spectrum would have to overlap almost perfectly. The complete lack of absorption in the near-infrared region would argue

against these long-lived states being excimers or other types of charge-transfer states.⁶² Since our time-resolved PL experiments also show no evidence for a large triplet population, there does not seem to be a reasonable candidate for this dark state.

On the other hand, the 1 ns TA spectrum bears a strong resemblance to what has been seen in polycrystalline pentacene films after 400 nm excitation. This derivative-like bleach feature has been assigned this line shape to a nonequilibrium heating effect rather than to overlapping bleach and excited-state absorption features.^{63,64} The basic idea is relatively simple. After the molecules relax nonradiatively, they deposit considerable energy into their environment and the local temperature can be much greater than the ambient temperature. The higher temperature typically leads to a blue shift of the S_0 – S_1 absorption spectrum. The differential absorption signal measures the difference between a cold (pump pulse off) and hot (pump pulse on) ground-state absorption, even in the absence of any excited-state population. If we assume that the entire energy of a 400 nm photon is temporarily localized within a region of 10 molecules, and assuming a heat capacity of 300 J/(mol K),⁶⁵ we estimate a local temperature rise on the order of 100–200 K. We have taken the absorption spectrum of a DIP thin film at elevated temperatures, with the results shown in Figure 9a. We can take the difference of the appropriately

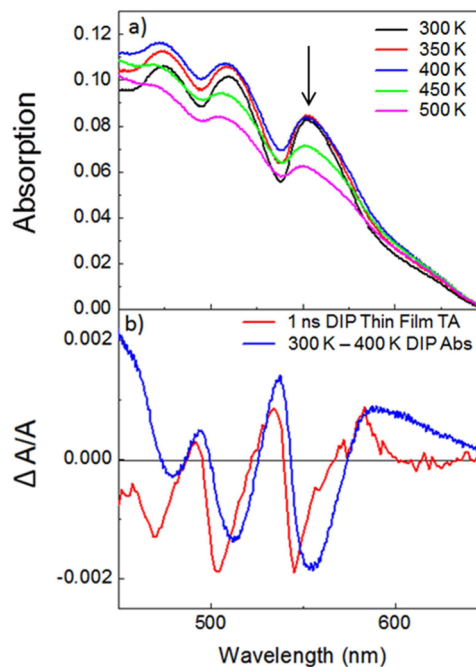


Figure 9. (a) Absorption spectra of a 100 nm thick DIP film at temperatures ranging from 300 to 500 K. The black arrow indicates direction of absorption feature evolution with increasing temperature. (b) The difference spectrum between 450 and 300 K absorption spectra (blue) overlaid with the 1 ns transient absorption spectrum of DIP thin film (red).

scaled 450 and 300 K absorption spectra and compare it to the 1 ns TA spectrum. The two spectra are overlaid in Figure 9b. The qualitative similarity of the two spectra suggests that a significant portion of the TA spectrum results from the hot ground state. By the same token, if we had decided to take the difference of the TA signal and the bleach signal calculated from the 300 K absorption spectrum in order to obtain the

induced absorption of the purported long-lived state, we would have obtained a spectrum very similar to the 450 K absorption, i.e., a shifted and broadened version of the 300 K absorption spectrum. This was in fact our first approach to analyzing the data, and it was the similarity of the S_0 – S_1 spectrum and calculated excited-state spectrum that motivated us to reanalyze our TA data in terms of thermal effects.

It should be emphasized that our estimate of a 150 K temperature jump is based on a qualitative comparison of the TA and absorption spectra and has considerable uncertainty. But this temperature rise is well within the range observed in other solid-state systems with chromophores that undergo rapid internal conversion.^{66,67} The transformation of photon energy into heat is a highly localized and transient process, since over the course of a few nanoseconds the heat will diffuse into the bulk sample, leading to a much smaller overall temperature rise. Typically even large transient temperature jumps do not lead to permanent sample damage.⁶⁸ DIP single crystals are known to undergo a polymorphic phase transition at 403 K,⁶⁹ but DIP thin films on gold have been found to be stable under sustained heating up to 150 °C,⁷⁰ comparable to our estimated temperature jump. Since no permanent changes in the optical properties of our samples were observed, we conclude that the main effect of the heating is to generate a transient hot ground-state absorption that masks the signatures of other residual long-lived excited states.

Our experimental results on solid DIP merit some discussion. We first consider the internal conversion process that returns the singlet excited state back to the ground state. If it is the same mechanism as for isolated DIP molecules in solution, then it must be accelerated by a factor of 5 in the solid film. But since molecular internal conversion is expected to be hindered in a constrained crystal environment, it is possible that this mechanism is no longer operative in the solid state. Theoretical work by Settels et al. has identified an alternative mechanism in which dimer states generate conical intersections that can provide fast pathways back to S_0 .⁷¹ They found that this mechanism was not effective in a pristine DIP crystal, but that it was very sensitive to intermolecular geometries and could become important at grain boundaries or defects. A logical source of grain boundaries would be between different regions of “standing up” and “lying down” molecules which are likely present in these films. Rapid migration of the initially created excitons to such interfaces could provide a physical explanation for the rapid internal conversion observed in our experiments. As discussed earlier, the morphology of DIP thin films is quite sensitive to preparation conditions (substrate, temperature), and differing concentrations of molecular packing motifs could lead to different lifetimes. The fact that our exciton lifetime is almost a factor of 2 longer than that observed by previous workers⁴⁷ suggests that a systematic study of how the exciton relaxation depends on material preparation conditions may yield even larger variations. Such a study is beyond the scope of the present work.

Rapid internal conversion in our films would suggest that most singlet excitons do not have the opportunity to diffuse over long distances before they relax back to the ground state. If this is the case, however, it is hard to understand the large (10–100 nm) exciton diffusion lengths reported for DIP.^{72–74} It is possible that the long-lived species observed in DIP's PL data may be responsible for photocurrent generation in OPV devices, but these long-lived emissive species represent only a small fraction of the total excitations. If all the emitting species

have similar radiative rates, making the amplitudes of the different exponential decays proportional to their associated populations, then they comprise 10% or less of the total excitations. However, external quantum yield spectra for DIP– C_{60} bilayer OPVs suggest that photoexcitation of the electron acceptor C_{60} plays an important role in generating photocurrent in these devices.^{75,76} This is consistent with our spectroscopic results showing that most photoexcited DIP molecules relax back to the ground state within a few hundred picoseconds. Photoexcited C_{60} molecules, on the other hand, can undergo rapid intersystem crossing to form long-lived triplet excitons with diffusion lengths exceeding 30 nm.^{77,78} DIP may be most useful as a charge transporting medium and as a way to induce order in neighboring thin films composed of other molecules, rather than as a source of ionizable mobile excitons. If this is the case, there is clearly room to optimize DIP's contribution to photocurrent generation.

CONCLUSIONS

We have studied the photophysical dynamics of the organic semiconductor molecule DIP in both dilute solution and in solid films. By itself, DIP in its excited singlet state undergoes a rapid (0.89 ns) internal conversion back to its ground state. In the solid-state samples studied here, multiple excited-state species are formed with lifetimes ranging from 170 ps to 6.5 ns. TA experiments indicate that the majority of the excited-state population undergoes internal conversion to form a hot ground state, leaving a minority of lower energy, longer-lived states. From the perspective of OPV applications, these results imply that it is difficult to generate large populations of long-lived mobile excitons in DIP thin films, given the preparation methods used in this paper. It is possible that chemical substitution or optimized preparation conditions could improve its excited-state lifetime while retaining its stability and crystalline order.

AUTHOR INFORMATION

Corresponding Author

*E-mail: christopher.bardeen@ucr.edu. Phone: 951-827-2723. Fax: 951-827-4713.

Present Address

§K.B.: Cavendish Laboratory, University of Cambridge, CB3 0HE Cambridge, United Kingdom.

Notes

The authors declare no competing financial interest.

ACKNOWLEDGMENTS

The authors acknowledge financial support from the National Science Foundation Grant CHE-1152677 (C.J.B.) and the German Research Foundation (BR 4869/1-1 and SCHR700/20-1).

REFERENCES

- (1) Koch, N. Organic Electronic Devices and Their Functional Interfaces. *ChemPhysChem* **2007**, *8*, 1438–1455.
- (2) Dürr, A. C.; Schreiber, F.; Munch, M.; Karl, N.; Krause, B.; Kruppa, V.; Dosch, H. High Structural Order in Thin Films of the Organic Semiconductor Diindenoperylene. *Appl. Phys. Lett.* **2002**, *81*, 2276–2278.
- (3) Dürr, A. C.; Schreiber, F.; Ritley, K. A.; Kruppa, V.; Krug, J.; Dosch, H.; Struth, B. Rapid Roughening in Thin Film Growth of an Organic Semiconductor (Diindenoperylene). *Phys. Rev. Lett.* **2003**, *90*, 016104–1/016104–3.

- (4) Barrera, E.; Oteyza, D. G. d.; Sellner, S.; Dosch, H.; Osso, J. O.; Struth, B. In Situ Study of the Growth of Nanodots in Organic Heteroepitaxy. *Phys. Rev. Lett.* **2006**, *97*, 076102–1/076102–4.
- (5) Zhang, X.; Barrera, E.; Goswami, D.; Oteyza, D. G. d.; Weis, C.; Dosch, H. Evidence For a Layer-Dependent Ehrlich-Schwobel Barrier in Organic Thin Film Growth. *Phys. Rev. Lett.* **2009**, *103*, 136101–1/136101–4.
- (6) Huang, H.; Huang, Y.; Pflaum, J.; Wee, A. T. S.; Chen, W. Nanoscale Phase Separation of a Binary Molecular System of Copper Phthalocyanine and Di-indenoperylene on Ag(111). *Appl. Phys. Lett.* **2009**, *95*, 263309–1/263309–3.
- (7) Kowarik, S.; Gerlach, A.; Sellner, S.; Cavalcanti, L.; Kononov, O.; Schreiber, F. Real-Time X-ray Diffraction Measurements of Structural Dynamics and Polymorphism in Diindenoperylene Growth. *Appl. Phys. A: Mater. Sci. Process.* **2009**, *95*, 233–239.
- (8) Heinemeyer, U.; Broch, K.; Hinderhofer, A.; Kytka, M.; Scholz, R.; Gerlach, A.; Schreiber, F. Real-Time Changes in the Optical Spectrum of Organic Semiconducting Films and Their Thickness Regimes During Growth. *Phys. Rev. Lett.* **2010**, *104*, 257401–1/257401–4.
- (9) Kowarik, S.; Gerlach, A.; Sellner, S.; Schreiber, F.; Cavalcanti, L.; Kononov, O. Real-Time Observation of Structural and Orientational Transitions During Growth of Organic Thin Films. *Phys. Rev. Lett.* **2006**, *96*, 125504–1/125504–4.
- (10) Scholz, R.; Gisslen, L.; Schuster, B.-E.; Casu, M. B.; Chasse, T.; Heinemeyer, U.; Schreiber, F. Resonant Raman Spectra of Diindenoperylene Thin Films. *J. Chem. Phys.* **2011**, *134*, 014504–1/014504–11.
- (11) Hinderhofer, A.; Hosokai, T.; Yonezawa, K.; Gerlach, A.; Kato, K.; Broch, K.; Frank, C.; Novak, J.; Kera, S.; Ueno, N.; Schreiber, F. Post-Growth Surface Smoothing of Thin Films of Diindenoperylene. *Appl. Phys. Lett.* **2012**, *101*, 033307–1/033307–4.
- (12) Aldahhak, H.; Matencio, S.; Barrera, E.; Ocal, C.; Schmidt, W. G.; Rauls, E. Structure Formation in Diindenoperylene Thin Films on Copper(111). *Phys. Chem. Chem. Phys.* **2015**, *17*, 8776–8783.
- (13) Wagner, J.; Gruber, M.; Hinderhofer, A.; Wilke, A.; Broker, B.; Frisch, J.; Amsalem, P.; Vollmer, A.; Opitz, A.; Koch, N.; et al. High Fill Factor and Open Circuit Voltage in Organic Photovoltaic Cells with Diindenoperylene as Donor Material. *Adv. Funct. Mater.* **2010**, *20*, 4295–4303.
- (14) Gruber, M.; Wagner, J.; Klein, K.; Hormann, U.; Opitz, A.; Stutzmann, M.; Brütting, W. Thermodynamic Efficiency Limit of Molecular Donor-acceptor Solar Cells and Its Application to Diindenoperylene/C₆₀-based Planar Heterojunction Devices. *Adv. Energy Mater.* **2012**, *2*, 1100–1108.
- (15) Gruber, M.; Rawolle, M.; Wagner, J.; Magerl, D.; Hormann, U.; Perlich, J.; Roth, S. V.; Opitz, A.; Schreiber, F.; Müller-Buschbaum, P.; et al. Correlating Structure and Morphology to Device Performance of Molecular Organic Donor-acceptor Photovoltaic Cells Based on Diindenoperylene (DIP) and C₆₀. *Adv. Energy Mater.* **2013**, *3*, 1075–1083.
- (16) Yu, S.; Opitz, A.; Grob, S.; Resel, R.; Oehzelt, M.; Brütting, W.; Salzmann, I.; Koch, N. Performance Enhancement of Diindenoperylene-Based Organic Photovoltaic Cells by Nanocolumn-arrays. *Org. Electron.* **2014**, *15*, 2210–2217.
- (17) Oteyza, D. G. d.; Barrera, E.; Dosch, H.; Ortega, J. E.; Wakayama, Y. Tunable Symmetry and Periodicity in Binary Supramolecular Nanostructures. *ChemPhysChem* **2011**, *13*, 4220–4223.
- (18) Aufderheide, A.; Broch, K.; Novak, J.; Hinderhofer, A.; Nervo, R.; Gerlach, A.; Banerjee, R.; Schreiber, F. Mixing-Induced Anisotropic Correlations in Molecular Crystalline Systems. *Phys. Rev. Lett.* **2012**, *109*, 156102–1/156102–5.
- (19) Hinderhofer, A.; Schreiber, F. Organic–Organic Heterostructures: Concepts and Applications. *ChemPhysChem* **2012**, *13*, 628–643.
- (20) Broch, K.; Aufderheide, A.; Raimondo, L.; Sassella, A.; Gerlach, A.; Schreiber, F. Optical Properties of Blends: Influence of Mixing-Induced Disorder in Pentacene:Diindenoperylene Versus Perfluoropentacene:Diindenoperylene. *J. Phys. Chem. C* **2013**, *117*, 13952–13960.
- (21) Broch, K.; Gerlach, A.; Lorch, C.; Dieterle, J.; Novak, J.; Hinderhofer, A.; Schreiber, F. Structure Formation in Perfluoropentacene:Diindenoperylene Blends and Its Impact on Transient Effects in the Optical Properties Studied in Real-Time During Growth. *J. Chem. Phys.* **2013**, *139*, 174709–1/174709–7.
- (22) Tucker, S. A.; Bates, H. C.; Amszi, V. L.; Acree, W. E.; Lee, H.; Raddo, P. D.; Harvey, R. G.; Fetzer, J. C.; Dyker, G. Spectroscopic Properties of Polycyclic Aromatic Compounds. Part II. Fluorescence Emission and Quenching Behavior of Select Acenaphthylene Derivatives in Organic Nonelectrolyte Solvents. *Anal. Chim. Acta* **1993**, *278*, 269–274.
- (23) Dunsbach, R.; Schmidt, R. Photophysical Properties of Some Polycyclic Conjugated Hydrocarbons Containing Five-Membered Rings. *J. Photochem. Photobiol., A* **1994**, *83*, 7–13.
- (24) Ahn, T. S.; Müller, A. M.; Al-Kaysi, R. O.; Spano, F. C.; Norton, J. E.; Beljonne, D.; Bredas, J. L.; Bardeen, C. J. Experimental and Theoretical Study of Temperature Dependent Exciton Delocalization and Relaxation in Anthracene Thin Films. *J. Chem. Phys.* **2008**, *128*, 054505/1–054505/11.
- (25) Katoh, R.; Suzuki, K.; Furube, A.; Kotani, M.; Tokumaru, K. Fluorescence Quantum Yield of Aromatic Hydrocarbon Crystals. *J. Phys. Chem. C* **2009**, *113*, 2961–2965.
- (26) Albrecht, W. G.; Coufal, H.; Haberkorn, R.; Michel-Beyerle, M. E. Excitation Spectra of Exciton Fission in Organic Crystals. *Phys. Status Solidi B* **1978**, *89*, 261–265.
- (27) Eaton, S. W.; Shoer, L. E.; Karlen, S. D.; Dyar, S. M.; Margulies, E. A.; Veldkamp, B. S.; Ramanan, C.; Hartzler, D. A.; Savikhin, S.; Marks, T. J.; et al. Singlet Exciton Fission in Polycrystalline Thin Films of a Slip-Stacked Perylene-dimide. *J. Am. Chem. Soc.* **2013**, *135*, 14701–14712.
- (28) Swenberg, C. E.; Stacy, W. T. Bimolecular Radiationless Transitions in Crystalline Tetracene. *Chem. Phys. Lett.* **1968**, *2*, 327–328.
- (29) Burdett, J. J.; Bardeen, C. J. The Dynamics of Singlet Fission in Crystalline Tetracene and Covalent Analogs. *Acc. Chem. Res.* **2013**, *46*, 1312–1320.
- (30) Jundt, C.; Klein, G.; Sipp, B.; Moigne, J. L.; Joucla, M.; Villaeys, A. A. Exciton Dynamics in Pentacene Thin Films Studied by Pump-Probe Spectroscopy. *Chem. Phys. Lett.* **1995**, *241*, 84–88.
- (31) Rao, A.; Wilson, M. W. B.; Hodgkiss, J. M.; Albert-Seifried, S.; Bassler, H.; Friend, R. H. Exciton Fission and Charge Generation Via Triplet Excitons in Pentacene/C₆₀ bilayers. *J. Am. Chem. Soc.* **2010**, *132*, 12698–12703.
- (32) Wilson, M. W. B.; Rao, A.; Clark, J.; Kumar, R. S. S.; Brida, D.; Cerullo, G.; Friend, R. H. Ultrafast Dynamics of Exciton Fission in Polycrystalline Pentacene. *J. Am. Chem. Soc.* **2011**, *133*, 11830–11833.
- (33) Heinemeyer, U.; Scholz, R.; Gisslen, L.; Alonso, M. I.; Osso, J. O.; Garriga, M.; Hinderhofer, A.; Kytka, M.; Kowarik, S.; Gerlach, A.; Schreiber, F. Exciton-Phonon Coupling in Diindenoperylene Thin Films. *Phys. Rev. B* **2008**, *78*, 085210–1/085210–10.
- (34) Nichols, V. M.; Rodriguez, M. T.; Piland, G. B.; Tham, F.; Nesterov, V. N.; Youngblood, W. J.; Bardeen, C. J. Assessing the Potential of Peropyrene as a Singlet Fission Material: Photophysical Properties in Solution and in the Solid State. *J. Phys. Chem. C* **2013**, *117*, 16802–16810.
- (35) Schael, F.; Lohmannsroben, H.-G. Photophysical Properties of the Non-Alternant Polycyclic Aromatic Hydrocarbons Periflanthene and 1,16-Benzoperiflanthene in Solution. *J. Photochem. Photobiol., A* **1992**, *69*, 27–32.
- (36) Kohler, B. E.; Spiglanin, T. A. Structure and Dynamics of Excited Singlet States of Isolated Diphenylhexatriene. *J. Chem. Phys.* **1984**, *80*, 5465–5471.
- (37) Jailaubekov, A. E.; Vengris, M.; Song, S.-H.; Kusumoto, T.; Hashimoto, H.; Larsen, D. S. Deconstructing the Excited-State Dynamics of b-Carotene in Solution. *J. Phys. Chem. A* **2011**, *115*, 3905–3916.
- (38) Casu, M. B.; Schuster, B.-E.; Biswas, I.; Raisch, C.; Marchetto, H.; Schmidt, T.; Chasse, T. Locally Resolved Core-hole Screening, Molecular Orientation, and Morphology in Thin Films of

Diindenoperylene Deposited on Au(111) Single Crystals. *Adv. Mater.* **2010**, *22*, 3740–3744.

(39) Krause, S.; Scholl, A.; Umbach, E. Interplay of Geometric and Electronic Structure in Thin Films of Diindenoperylene on Ag(111). *Org. Electron.* **2013**, *14*, 584–590.

(40) Huang, Y. L.; Chen, W.; Huang, H.; Qi, D. C.; Chen, S.; Gao, Y. Y.; Pflaum, J.; Wee, A. T. S. Ultrathin Films of Diindenoperylene on Graphite and SiO₂. *J. Phys. Chem. C* **2009**, *113*, 9251–9255.

(41) Dürr, A. C.; Nickel, B.; Sharma, V.; Taffner, U.; Dosch, H. Observation of Competing Modes in the Growth of Diindenoperylene on SiO₂. *Thin Solid Films* **2006**, *503*, 127–132.

(42) Heinemeyer, U.; Hinderhofer, A.; Alonso, M. I.; Osso, J. O.; Garriga, M.; Kytka, M.; Gerlach, A.; Schreiber, F. Uniaxial Anisotropy of Organic Thin Films Determined by Ellipsometry. *Phys. Status Solidi A* **2008**, *205*, 927–930.

(43) Zhang, D.; Horneber, A.; Mihaljevic, J.; Heinemeyer, U.; Braun, K.; Schreiber, F.; Scholz, R.; Meixner, A. J. Plasmon Resonance Modulated Photoluminescence and Raman Spectroscopy of Diindenoperylene Organic Semiconductor Thin Film. *J. Lumin.* **2011**, *131*, 502–505.

(44) Meinardi, F.; Cerninara, M.; Sassella, A.; Borghesi, A.; Spearman, P.; Bongiovanni, G.; Mura, A.; Tubino, R. Intrinsic Exciton Luminescence in Odd and Even Numbered Oligothiophenes. *Phys. Rev. Lett.* **2002**, *89*, 157403–1/157403/4.

(45) Spano, F. C. Excitons in Conjugated Oligomer Aggregates, Films and Crystals. *Annu. Rev. Phys. Chem.* **2006**, *57*, 217–243.

(46) Spano, F. C. The Spectral Signatures of Frenkel Polarons in H- and J-aggregates. *Acc. Chem. Res.* **2010**, *43*, 429–439.

(47) Heilig, M.; Domhan, M.; Port, H. Optical Properties and Morphology of Thin Diindenoperylene Films. *J. Lumin.* **2004**, *110*, 290–295.

(48) Pope, M.; Swenberg, C. E. *Electronic Processes in Organic Crystals and Polymers*; Oxford University Press: New York, 1999.

(49) Smith, M. B.; Michl, J. Singlet Fission. *Chem. Rev.* **2010**, *110*, 6891–6936.

(50) Geacintov, N.; Pope, M.; Vogel, F. Effect of Magnetic Field on the Fluorescence of Tetracene Crystals: Exciton Fission. *Phys. Rev. Lett.* **1969**, *22*, 593–596.

(51) Burdett, J. J.; Piland, G. B.; Bardeen, C. J. Magnetic Field Effects and the Role of Spin States in Singlet Fission. *Chem. Phys. Lett.* **2013**, *585*, 1–10.

(52) Burdett, J. J.; Müller, A. M.; Gosztola, D.; Bardeen, C. J. Excited State Dynamics in Solid and Monomeric Tetracene: the Roles of Superradiance and Exciton Fission. *J. Chem. Phys.* **2010**, *133*, 144506/1–144506/12.

(53) Burdett, J. J.; Gosztola, D.; Bardeen, C. J. The Dependence of Singlet Exciton Relaxation on Excitation Density and Temperature in Polycrystalline Tetracene Thin Films: Kinetic evidence for a dark intermediate state and implications for singlet fission. *J. Chem. Phys.* **2011**, *135*, 214508/1–214508/10.

(54) Fielding, P. E.; Jarnagin, R. C. “Excimer” and “Defect” Structure for Anthracene and Some Derivatives in Crystals, Thin Films, and Other Rigid Matrices. *J. Chem. Phys.* **1967**, *47*, 247–252.

(55) Horiguchi, R.; Iwasaki, N.; Maruyama, Y. Time-Resolved and Temperature-Dependent Fluorescence Spectra of Anthracene and Pyrene in Crystalline and Liquid States. *J. Phys. Chem.* **1987**, *91*, 5135–5139.

(56) Campillo, A. J.; Hyer, R. C.; Shapiro, S. L.; Swenberg, C. E. Exciton interactions in crystalline tetracene studied by single picosecond pulse excitation. *Chem. Phys. Lett.* **1977**, *48*, 495–500.

(57) Yago, T.; Tamaki, Y.; Furube, A.; Katoh, R. Self-Trapping Limited Exciton Diffusion in a Monomeric Perylene Crystal as Revealed by Femtosecond Laser Absorption Microscopy. *Phys. Chem. Chem. Phys.* **2008**, *10*, 4435–4441.

(58) Greene, B. I.; Millard, R. R. Singlet-Exciton Fusion in Molecular Solids: a Direct Subpicosecond Determination of the Time-Dependent Annihilation Rates. *Phys. Rev. Lett.* **1985**, *55*, 1331–1334.

(59) Lim, S. H.; Bjorklund, T. G.; Spano, F. C.; Bardeen, C. J. Exciton Delocalization and Superradiance in Tetracene Thin Films and Nanoaggregates. *Phys. Rev. Lett.* **2004**, *92*, 107402/1–107402/4.

(60) Voigt, M.; Langner, A.; Schouwink, P.; Lupton, J. M.; Mahrt, R. F.; Sokolowski, M. Picosecond Time Resolved Photoluminescence Spectroscopy of a Tetracene Film on Highly Oriented Pyrolytic Graphite: Dynamical Relaxation, Trap Emission, and Superradiance. *J. Chem. Phys.* **2007**, *127*, 114705/1–114705/8.

(61) Camposeo, A.; Polo, M.; Tavazzi, S.; Silvestri, L.; Spearman, P.; Cingolani, R.; Pisignano, D. Polarized Superradiance From Delocalized Exciton Transitions in Tetracene Single Crystals. *Phys. Rev. B* **2010**, *81*, 033306/1–033306/4.

(62) Katoh, R.; Katoh, E.; Nakashima, N.; Yuuki, M.; Kotani, M. Near-IR Absorption Spectrum of Aromatic Excimers. *J. Phys. Chem. A* **1997**, *101*, 7725–7728.

(63) Albert-Seifried, S.; Friend, R. H. Measurement of Thermal Modulation of Optical Absorption in Pump-Probe Spectroscopy of Semiconducting Polymers. *Appl. Phys. Lett.* **2011**, *98*, 223304–1/223304–3.

(64) Rao, A.; Wilson, M. W. B.; Albert-Seifried, S.; Petro, R. D.; Friend, R. H. Photophysics of Pentacene Thin Films: the Role of Exciton Fission and Heating Effects. *Phys. Rev. B* **2011**, *84*, 195411–1/195411–8.

(65) Fulem, M.; Lastovka, V.; Straka, M.; Ruzicka, K.; Shaw, J. M. Heat Capacities of Tetracene and Pentacene. *J. Chem. Eng. Data* **2008**, *53*, 2175–2181.

(66) Wen, X.; Tolbert, W. A.; Dlott, D. D. Ultrafast Temperature Jump in Polymers: Phonons and Vibrations Heat up at Different Rates. *J. Chem. Phys.* **1993**, *99*, 4140–4151.

(67) Mohammed, O. F.; Samartzis, P. C.; Zewail, A. H. Heating and Cooling Dynamics of Carbon Nanotubes Observed by Temperature-Jump Spectroscopy and Electron Microscopy. *J. Am. Chem. Soc.* **2009**, *131*, 16010–16011.

(68) Chen, S.; Lee, I.-Y. S.; Tolber, W. A.; Wen, X.; Dlott, D. D. Applications of Ultrafast Temperature Jump Spectroscopy to Condensed Phase Molecular Dynamics. *J. Phys. Chem.* **1992**, *96*, 7178–7186.

(69) Heinrich, M. A.; Pflaum, J.; Tripathi, A. K.; Frey, W.; Steigerwald, M. L.; Siegrist, T. Enantiotropic Polymorphism in Diindenoperylene. *J. Phys. Chem. C* **2007**, *111*, 18878–18881.

(70) Dürr, A. C.; Schreiber, F.; Kelsch, M.; Carstanjen, H. D.; Dosch, H. Morphology and Thermal stability of Metal Contacts on Crystalline Organic Thin Films. *Adv. Mater.* **2002**, *14*, 961–963.

(71) Settels, V.; Schubert, A.; Tafipolski, M.; Liu, W.; Stehr, V.; Topczak, A. K.; Pflaum, J.; Deibel, C.; Fink, R. F.; Engel, V.; Engels, B. Identification of Ultrafast Relaxation Processes as a Major Reason for Inefficient Exciton Diffusion in Perylene-Based Organic Semiconductors. *J. Am. Chem. Soc.* **2014**, *136*, 9327–9337.

(72) Kurlle, D.; Pflaum, J. Exciton Diffusion Length in the Organic Semiconductor Diindenoperylene. *Appl. Phys. Lett.* **2008**, *92*, 133306–1/133306–3.

(73) Rim, S.-B.; Peumans, P. The Effects of Optical Interference on Exciton Diffusion Length Measurements Using Photocurrent Spectroscopy. *J. Appl. Phys.* **2008**, *103*, 124515–1/124515–5.

(74) Lunt, R. R.; Giebink, N. C.; Belak, A. A.; Benziger, J. B.; Forrest, S. R. Exciton Diffusion Lengths of Organic Semiconductor Thin Films Measured by Spectrally Resolved Photoluminescence Quenching. *J. Appl. Phys.* **2009**, *105*, 053711–1/053711–7.

(75) Steindamm, A.; Brendel, M.; Topczak, A. K.; Pflaum, J. Thickness Dependent Effects of an Intermediate Molecular Blocking Layer on the Optoelectronic Characteristics of Organic Bilayer Photovoltaic Cells. *Appl. Phys. Lett.* **2012**, *101*, 143302–1/143301–4.

(76) Zhou, Y.; Taima, T.; Kuwabara, T.; Takahashi, K. Efficient Small-Molecule Photovoltaic Cells Using a Crystalline Diindenoperylene Film as a Nanostructured Template. *Adv. Mater.* **2013**, *25*, 6069–6075.

(77) Peumans, P.; Yakimov, A.; Forrest, S. R. Small Molecular Weight Organic Thin-Film Photodetectors and Solar Cells. *J. Appl. Phys.* **2003**, *93*, 3693–3723.

(78) Qin, D.; Gu, P.; Dhar, R. S.; Razavipour, S. G.; Ban, D. Measuring the Exciton Diffusion Length of C₆₀ in Organic Planar Heterojunction Solar Cells. *Phys. Status Solidi A* **2011**, *208*, 1967–1971.